AIAA-2004-2256

2-D, BLUFF BODY DRAG ESTIMATION USING A GREEN'S FUNCTION/GRAM-CHARLIER SERIES APPROACH

Lawrence J. De Chant[1]
Sandia National Laboratories,
Albuquerque, NM, 87185-0825

In this study, we extend self-similar, far-field, turbulent wake concepts to estimate the 2-d drag coefficient for a range of bluff body problems. The self-similar wake velocity defect that is normally independent of the near field wake (and hence body geometry) is modified using a combined approximate Green's function/Gram-Charlier series approach to retain the body geometry information. Formally a near field velocity defect profile is created using small disturbance theory and the inviscid flow field associated with the body of interest. The defect solution is then used as an initial condition in the approximate Green's function solution. Finally, the Green's function solution is matched to the Gram-Charlier series yielding profiles that are integrated to yield the net form drag on the bluff body. Preliminary results indicate that drag estimates computed using this method are within approximately 15% as compared to published values for flows with large separation. This methodology may be of use as a supplement to CFD and experimental solutions in reducing the heavy computational and experimental burden of estimating drag coefficients for blunt body flows for preliminary design type studies.

1. Introduction

Drag estimates for strongly separated flow over blunt bodies is an essential piece of information for many engineering systems. An application that demands our particular attention is aerodynamic drag forces on large ground transportation vehicles, i.e. tractor/trailer trucks. As noted by Roy et. al[1] for a common tractor/trailer, energy losses due to rolling resistance and accessories increase linearly with vehicle speed, while energy losses due to aerodynamic drag increase with the cube of the speed. At a typical highway speed of 70 mph, aerodynamic drag accounts for approximately 65% of the energy output of the engine[2]. Due to the large number of tractor/trailers on the US highways, even modest reductions in aerodynamic drag can significantly reduce domestic fuel consumption.

Lawrence J. De Chant; Ph.D. Senior Staff Member, Current address: Sandia National Laboratories, P.O. 5800, Albuquerque, NM 87185-0825; 505-844-4250, ljdecha@sandia.gov

Sandia is a multiprogram laboratory operated by Sandia Corporation, a Lockheed Martin Company, for the United States Department of Energy's National Nuclear Security Administration under contract DE-AC04-94AL85000.

Though most modern computationally based aerodynamic drag reduction studies have focused on Computational Fluid Dynamics (CFD) methods utilizing evermore sophisticated (and concurrently computationally expensive) methodologies, there remains a valuable role for reduced complexity, analytically based models. Here we describe a model that modifies the classical self-similar turbulent wake models discussed by Tennekes and Lumley[3] and Townsend[4]. As such, we will start by describing the Tennekes and Lumley self-similar analysis, identifying its limitations and then suggest an alternative approach based upon a combination of inviscid flow field modeling, a Green's function solution and association with Gram-Charlier series. Although our focus is on 2d bluff body drag, the methods presented are extensible to axisymmetric and 3-d flow.

2. 2-d Bluff Body Drag

Using order of magnitude arguments Tennekes and Lumley[3] show that a suitable momentum equation for turbulent 2-d wakes is given by:

$$U\frac{\partial U}{\partial x}+\frac{\partial}{\partial y}\left(\overline{uv}\right)=0 \qquad (1)$$

where U denotes the Reynolds averaged mean velocity and u and v represent the streamwise and

cross-stream fluctuating components, respectively. To the same order of magnitude one may linearize to obtain:

$$U_0 \frac{\partial U}{\partial x} + \frac{\partial}{\partial y}\left(\overline{uv}\right) = 0 \quad ; \quad uv \propto \frac{\partial U}{\partial y} \qquad (2)$$

where U_0 is the free stream velocity in the streamwise or x-direction.

To reduce equation (2), Tennekes and Lumley argue that there must be a self-preservation solution, e.g. self-similar construction for the velocity field, i.e.:

$$\frac{U_0 - U}{U_s} = f\left(\frac{y}{l}\right) \qquad (3)$$

is necessary where U_s is the maximum cross-stream variation in U. Note, that for wakes U_s will be U(y=0) where the relevant coordinate system and associated definitions are shown in figure 1.

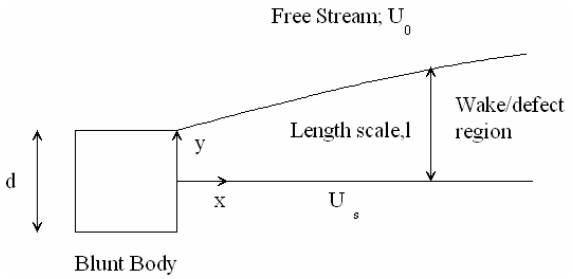

Figure 1 Schematic diagram of wake flow with coordinate, velocity and length scale definitions.

Unfortunately, the solution obtained by Tennekes and Lumley, cannot be strictly valid in the near field since the form of the similarity solution chosen by Tennekes and Lumley[3] requires that $U_s = Ax^{-1/2}$ $l = Bx^{1/2}$ and A and B are constants to be determined. Obviously, the U_s solution is not (and cannot be) valid for x<<1. This limitation poses no problem in the far-field, of course, and is acceptable in an intermediate overlap region as well, but cannot be applied in the wake near-field.

The connection to the velocity defect field and the drag coefficient is given by (2-d drag coefficient); equation:

$$C_D = 2\frac{\theta}{d} = \int_{-\infty}^{\infty} f d\eta \qquad (4)$$

The 2-d momentum thickness θ is introduced through equation (4) as well. See Tennekes and Lumley (1974) for details.

3. Approximate Green's function solution

An alternative approach to the physically based similarity arguments presented in the text involves the mathematical analysis of a generalized problem. Here we discuss a range of fundamental solutions to the heat equation (the canonical form of the linearized wake relationship).

The heat (linearized wake) equation may be written (α_0 is a constant):

$$\frac{\partial u}{\partial x} = \alpha_0^2 \frac{\partial^2 u}{\partial y^2} \qquad (5)$$

where we have the boundary conditions, $u(x, y \to \infty) = \left.\frac{\partial u}{\partial y}\right|_{y=0} = 0$. The initial condition is not specified, but is reflected by an additional boundary constraint. Introducing a set of generalized variables we write $u = x^a f(\eta)$; $\eta = yx^b$. Performing the necessary change of variable yields the relationship:

$$x^{a-1}\left(b\eta f' + af\right) = \alpha_0^2 x^{a+2b} f'' \qquad (6)$$

Similarity can be achieved by letting b=-1/2 with the coefficient an arbitrary. It is of interest to consider two possible cases; (1) a=b=-1/2 and (2) a=0, b=-1/2 (classical Boltzmann transformation[5]). The term α_0 is chosen to yield simple coefficients. The two solutions are:
case (1), a=b=-1/2

$$f'' + \eta f' + f = 0 \quad ; \quad f = \exp\left(-1/2\eta^2\right) \qquad (7)$$

and case (2)) a=0, b=-1/2

$$f'' + \eta f' = 0 \quad ; \quad f = 1 - erf\left(\sqrt{2}/2\eta\right) \qquad (8)$$

Note that both solutions satisfy the boundary constraint f(η)=1 and the far field boundary condition

f(η→∞)=0. However, the second solution, i.e. equation (8), cannot satisfy symmetry, f'(0)=0, a reflection that the choice given for equation (7) is the "correct" one, while the Boltzmann transformation is not a satisfactory solution.

However the choice a=0, b=-1/2 (classical Boltzmann transformation) is related to a Green's function solution to equation (5)[6]. The Green's function solution (can be solved via Laplace/Cosine transforms as well) to equation (5) is:

$$u(x,y)=\frac{1}{\sqrt{4\pi\alpha_0^2 x}}\int_0^\infty u(0,\bar{y})\left[\begin{array}{l}\exp\left(-\frac{(y-\bar{y})^2}{4\alpha_0^2 x}\right)\\+\exp\left(-\frac{(y+\bar{y})^2}{4\alpha_0^2 x}\right)\end{array}\right]d\bar{y} \tag{9}$$

Though equation (9) satisfies equation (5), it is clearly not a self-similar solution. An interesting special case for this problem results if we let u(x,0) be the unit step function, u(0,y)=1 for 0<y<1 and zero otherwise. Substitution into equation (9) gives:

$$u(x,y)=\frac{1}{2}\left[erf\left(\frac{(y+1)}{\sqrt{4\alpha_0^2 x}}\right)-erf\left(\frac{(y-1)}{\sqrt{4\alpha_0^2 x}}\right)\right] \tag{10}$$

which, again, cannot be self-similar. A self-similar equation is possible if we let u(x=0,y)=δ(y) where δ denotes the Dirac delta function. The solution associated with the point source is related to equation (7). Thus we note that there is only a very limited initial condition form that is supported by the self-similar relationships. If, however we are willing to use the functional form of equation (9) we can form a solution to the governing equations that is self-similar, i.e.

$$f_{GF}(\eta)=\frac{1}{\sqrt{\pi}}\int_0^\infty f_{near}(\bar{\eta})\left[\begin{array}{l}\exp\left(-(\eta_0+\bar{\eta})^2\right)+\\\exp\left(-(\eta_0-\bar{\eta})^2\right)\end{array}\right]d\bar{\eta} \tag{11}$$

where η_0 denotes the dimensionless length scale associated with the bluff body. Note, that equation (11) will approximately satisfy the full range of conditions required for solution of the wake problem, i.e. approximately satisfies equation (6), recovers symmetry, f'(0)=0 and satisfies the far-field conditions f(η→∞)=0.

4. "Initial Condition Velocity Field"; Connection to the Inviscid Flow Field

To utilize equation (11) to obtain the defect velocity field, it is necessary to be able to compute a near field velocity defect profile, i.e. f_{near}. This function must provide the sum total of the bluff bodies geometric information. In terms of a practical result, it also must be readily obtainable and unique. Perhaps the most obvious closure for the near field defect solution that satisfies these requirements is to utilize the local inviscid potential flow solution.

For sharp edged bluff bodies such as the square cylinder shown in figure 1. where the separation location is well established, the defect velocity field is readily estimated by the discontinuous step function:

$$f_{near}=\begin{cases}1 & 0\le\eta\le 1\\ 0 & otherwise\end{cases};\qquad \text{where}\quad \eta=2y/d.$$

Substitution of this near-field relationship into equation (11) yields: $f_{GF}=\frac{\left[erf(\eta+1)-erf(\eta-1)\right]}{2}$. Notice, that when integrated the near field and Green's function solution, give $C_{D=}\int_{-\infty}^{\infty} f_{near}\,d\eta=\int_{-\infty}^{\infty} f\,d\eta=2$. Though this estimate for 2-d drag is quite good, since $C_{D,exper}=2.1$[7], we note that the Green's function does not modify the net initial defect velocity, hence in terms of the drag coefficient the Green's function relationship provides no new information. Our reason to utilize the Green's function form will become apparent later, but we already note, that the Green's function relationship will satisfy several essential properties including:

continuous, differentiable flow field valid over full domain, i.e. -∞→+∞.

satisfies symmetry and far field boundary conditions

and, approximately, satisfies governing linearized, momentum (diffusion) equation.

When considering a smooth bluff body such as a circular cylinder it is necessary to modify our methodology. The inviscid defect velocity for a circular cylinder can be approximated as: $f_{near}=\frac{1-\eta^2}{\left(1+\eta^2\right)^2}$. From figure 2. we note that the integral for

$$\int_{-\infty}^{\infty} \frac{1-\eta^2}{\left(1+\eta^2\right)^2} d\eta =$$

$$\int_{-\infty}^{\infty} \frac{1}{\sqrt{\pi}} \int_{0}^{\infty} \frac{1-\overline{\eta}}{(1+\overline{\eta}^2)^2}^2 \left[\begin{matrix} \exp\left(-(\eta+\overline{\eta})^2\right)+ \\ \exp\left(-(\eta-\overline{\eta})^2\right) \end{matrix} \right] d\overline{\eta}\, d\eta = 0$$

, implying that the inviscid net drag on cylinder is zero (as is well known by D'Alembert's paradox). Our focus, here should be on the core (close to centerline) velocity defect. Thus if one considers f_{near} near the centerline only we write:

$$f_{near} = \begin{cases} 1-\eta^2 & 0 \le \eta \le 1 \\ 0 & otherwise \end{cases}.$$

The piecewise continuous field is constructed such that $f_{near}>0$. This simple relationship is precisely that one utilized for laminar flow (laminar on the body surface, the wake is always turbulent) over a cylinder.

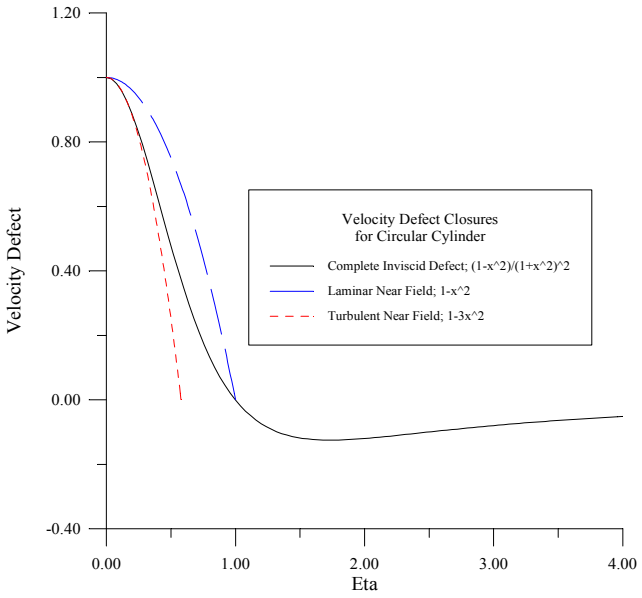

Figure 2. Local defect velocity field approximation for flow in the lee of a circular cylinder.

For higher Reynolds flows, e.g. turbulent surface flow over a cylinder, it is necessary to modify the preceding methodology. In this situation, it is necessary to utilize a more complete near field approximation, i.e. by expanding the complete defect velocity relationship in Taylor series we can write: $\frac{1-\eta^2}{\left(1+\eta^2\right)^2} \approx 1-3\eta^2+\ldots$. Thus, constructing a piecewise continuous near field defect velocity relationship we write:

$$f_{near} = \begin{cases} 1-3\eta^2 & 0 \le \eta \le 1/\sqrt{3} \\ 0 & otherwise \end{cases}.$$

Other examples of near field expansions are provided subsequently. We note, that our attention is directed towards bluff body flows where we must assume that massive separation has occurred. Sharp (minimal rounding as compared to body length scales) edged flow geometries will tend to exhibit this type of separation. Flows where separation is long delayed (very smooth well-rounded shapes with highly turbulent surface flow, e.g. high Reynolds number circular cylinder) will tend to be difficult to model using the described methodology. For these situations, we can expect qualitative agreement only.

5. Gram-Charlier Series

In the previous section, it was clear that it is the local velocity defect solution that provides an estimate of drag since the Green's function relationship, equation (11), preserves the area under the local velocity defect approximation. However, the classical far-field wake profiles derived by Tennekes and Lumley should be taken into account in any formulation. The far-field defect profile solution consistent with the Tennekes and Lumley formulation is given as: $f_{near} = \exp\left(-\frac{1}{2}\alpha\eta^2\right)$. This function positive over the entire half space, thus the relationship is continuous. By way of comparison the drag coefficient integral using this value (or its Green's function form) is:

$$C_D = \int_{-\infty}^{\infty} \exp\left(-\frac{1}{2}\alpha\eta^2\right) d\eta = \sqrt{2\pi}$$ that is approximately 25% larger than the flow over a 2-d square cylinder. This value represents a maximum drag for typical 2-d bodies. Thus, we probably would not prefer to use the far-field wake directly in a drag estimation scheme.

However, as noted by Tennekes and Lumley[3], the far field wake might represent a single first term in a Gram-Charlier series (see http://mathworld.wolfram.com/CharlierSeries.html, Keeney and Keeping[7]; Cramer[8] for a summary concerning Gram-Charlier series), where the series is written:

$$f(\eta) = a_0 \exp\left(-\frac{1}{2}\eta^2\right) + a_1 \frac{d}{d\eta}\left[\exp\left(-\frac{1}{2}\eta^2\right)\right] + a_2 \frac{d^2}{d\eta^2}\left[\exp\left(-\frac{1}{2}\eta^2\right)\right] + \ldots \quad (12)$$

with the new, unknown coefficients, a_i. The question now becomes, how does one assess these constants. We propose, that the constants a_i, be related to the Green's function flow fields that have been described previously (see equation (11)).

Demanding matching of the functional values and the derivatives between the Green's function solution and the Gram-Charlier expansion will uniquely specify the constants, a_i in equation (12). It is convenient to rewrite equation (13) in the form:

$$f(\eta) = a_0 \exp\left(-\frac{1}{2}\eta^2\right) - a_1\eta\left[\exp\left(-\frac{1}{2}\eta^2\right)\right] - a_2(1-\eta^2)\left[\exp\left(-\frac{1}{2}\eta^2\right)\right] + \ldots \quad (13)$$

Computing derivatives, evaluating and collecting terms, we write:

$$\begin{aligned} f_{GF}(0) &= a_0 - a_2 \\ f'_{GF}(0) &= -a_1 \\ f''_{GF}(0) &= 3a_2 - a_1 - a_0 \end{aligned} \quad (14)$$

Notice that for symmetric problems (the possibility of asymmetry is included in the complete series) that we can write $a_0 = \frac{1}{2}(3f_{GF}(0) - f''_{GF}(0))$.

It is worth stating that the Gram-Charlier series is only convergent for rapidly decaying kernel functions and thus is not typically convergent[8]. The utility of divergent asymptotic series, however, is well known in general[9] and noted for Gram-Charlier series by Cramer[8].

With the coefficients in equation (12) or equivalently, equation (13) specified, we introduce the new profile information into the force balance relationship, e.g. equation (4), where we note, that the integrals are given by $\int_{-\infty}^{\infty} \exp(-\frac{1}{2}\eta^2)d\eta = (2\pi)^{1/2}$ and $\int_{-\infty}^{\infty} \eta^2 \exp(-\frac{1}{2}\eta^2)d\eta = (2\pi)^{1/2}$. Notice, however that since $\int_{-\infty}^{\infty}(1-\eta^2)\left[\exp\left(-\frac{1}{2}\eta^2\right)\right]d\eta = 0$, the contribution from the second derivative term does not effect the remainder of the solution. The integral associated with the a_1 term (necessary for non-symmetric problems) is given by $\int_{-\infty}^{\infty} \exp(-\frac{1}{2}\eta^2)\eta d\eta = 1$.

b

From these equations, it is possible to obtain values, equivalent to equation (11) for both the "square cylinder" and the circular cylinder wakes. As a simple example (minimal algebraic complexity) we consider the square cylinder. Utilizing the discontinuous step function defect velocity field, $f_{near} = \begin{cases} 1 & 0 \le \eta \le 1 \\ 0 & otherwise \end{cases}$; where $\eta=2y/d$ we use the Green's function relationship, equation (11), to write: $f = \frac{[erf(\eta+1) - erf(\eta-1)]}{2}$.

Computing the necessary derivative evaluations (note that we use the symbolic solver MAPLE ™ to perform many of the straightforward but tedious operations in this process):

$$\begin{aligned} f_{GF}(0) &= erf(1) \approx 0.84 \\ f'_{GF}(0) &= 0 \\ f''_{GF}(0) &= -4e^{-1}/\sqrt{\pi} \approx -0.83 \end{aligned} \quad (15)$$

Thus $a_0 = \frac{1}{2}(3f_{GF}(0) - f''_{GF}(0)) \approx 0.84$, implying that $C_D = 0.85(2\pi)^{1/2} = 2.10$.

4. Preliminary Results

Preliminary drag coefficient results for a range of 2-d bluff body shapes are presented in table 1. Comparison is made with published values given in White[10] and Hughes and Brighton[11].

Shape	Theor. C_D	Pub. C_D	Reynolds #	Relative Error (%)
Square Cylinder (step function)	2.1	2.1	Independent	0%
2:1 Rectangular Cylinder (num. inviscid)	1.85	1.7	Independent ($Re>10^3$)	10%
Equilateral triangle (apex facing flow)**	1.35	1.6	Independent	15%
Circular Cylinder (laminar B. L.)	1.3	1.2	$10^3<Re<10^5$	8%
Circular Cylinder (Transition B. L.)	0.63	0.6	$Re\approx 5x10^5$	5%
Circular Cylinder (Turbulent B. L.)***	0.51	0.3	$Re>10^6$	70%
Parabolic Cylinder, f=x(1-x) (Small disturbance)(Turbulent B. L.)	0.15	0.2	Re>>>1	25%

Table 1 Preliminary comparison between published 2-d drag coefficient results and the theoretically-based model developed here. Notice that the theoretical model compares adequately with published values for rapidly separated flows (sharp edged and laminar) but performs poorly for smooth bodies with delayed separation.

*A comparison between numerically derived inviscid and step function velocity defect relationships is shown in figure 3 for a 2-d rectangular cylinder.

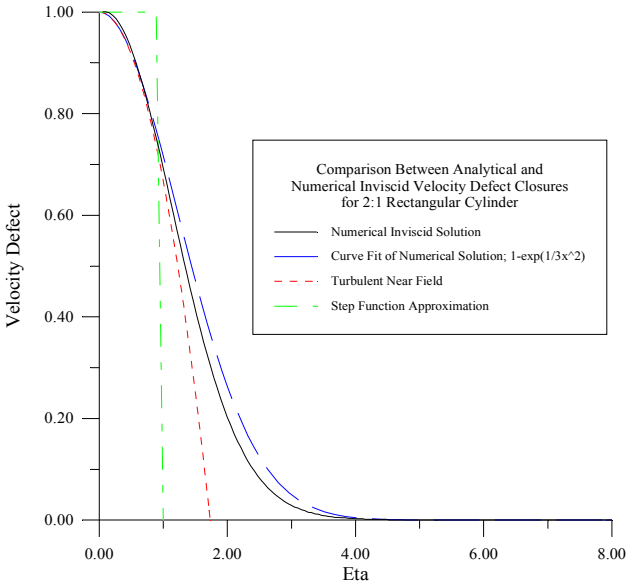

Figure 3. Numerically generated inviscid flow velocity defect function for 2:1 rectangular cylinder.

**Simple step function closure;

$$f_{near} = \begin{cases} 1 & 0 \le \eta \le \sqrt{2}/2 \\ 0 & otherwise \end{cases}$$

***An 80% effective diameter approximation has been used in this computation, see below for details.

Recall, that a requirement of this model is that the flow field be characterized by large-scale separation. The less energetic, locally laminar model (the wake is turbulent regardless of the character, laminar or turbulent, of the local flow on the body), however, will rapidly separate thereby creating a flow that is better described by the theoretical model. Additionally, the use of a turbulent length scale that is on the order of the thickness of the body, i.e. $l \approx d/2$ becomes rather less meaningful for a smooth flow with delayed separation, a more appropriate value for the length scale is to use the separation point over the body to compute an effective diameter. For a circular cylinder separating at approximately 120 degrees[12]) the effective diameter is estimated to be approximately 80% of the true diameter. (See figure 4).

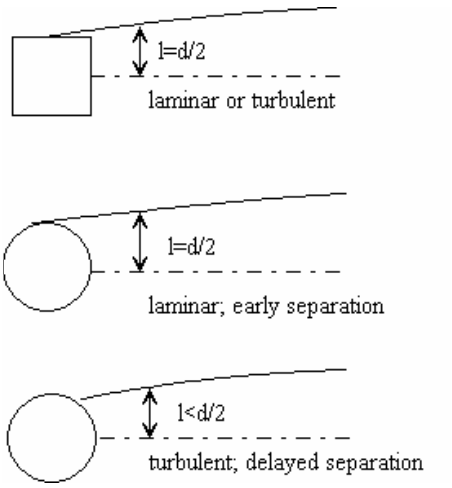

Figure 4. Effect of rounding and boundary layer type (laminar or turbulent) on the validity of length scale assignment assumption for square and circular cylinders. Notice that $l \approx d/2$ is a particularly poor approximation for turbulent flow over a cylinder.

Though our interest is primarily focused upon deriving an estimate for the integrated value C_D, we can also utilize the preceding analysis to obtain estimates of the flow field behavior. Following

Tennekes and Lumley[3], and utilizing their variables $U_s = Ax^{-1/2}$ $l = Bx^{1/2}$ and A and B are constants to be determined we obtain an approximation for the centerline velocity behavior as a function of x: $U_s = 3.16U_0 dx^{-1}$. Of course, this expression is not valid for x<<1, but we expect that the functional form, i.e. power of x, -1 to be correct. By way of comparison, we consider the centerline velocity data for flow over a square cylinder square cylinder given by Lyn et. al[13]. in figure 5.

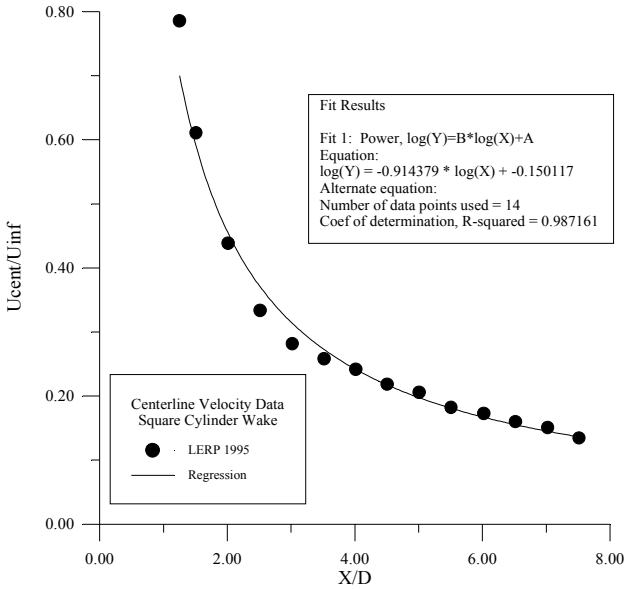

Figure 5. Centerline velocity data for flow over a square cylinder square cylinder given by Lyn et. al.[10] with regression analysis. Notice that the curve-fit expression decays to the –0.91 power a value that compares well with the theoretical value, -1.

6. Conclusions and recommendations

In this discussion we have modified classical self-similar, far-field, turbulent wake concepts to estimate the 2-d drag coefficient for a range of bluff body problems. The self-similar wake velocity defect that would be normally independent of the near field wake (and hence body geometry) was altered using a combined approximate Green's function/Gram-Charlier series approach to retain the body geometry information. Preliminary results indicate that drag estimates computed using this method are within approximately 10-20% as compared to published values for flows with large separation. The potential value of this method is as a way to utilize poorly resolved simulation results to provide an inexpensive estimate of body drag or as the basis of a physically consistent correlation scheme. This methodology may be of use as a supplement to CFD and experimental solutions in reducing the heavy computational and experimental burden of estimating drag coefficients for blunt body flows for preliminary design type studies.

7. Acknowledgements

The author would like thank professor C. Roy, Auburn University, AL; Dr. B. Hassan, Dr. M. Barone, Dr. F. Blottner and J. Payne, Sandia National Laboratories, NM for their continued technical support. Sandia is a multi-program Laboratory operated by Sandia Corporation, a Lockheed Martin Company, for the United States Department of Energy under contract DE-AC04-94-AL85000.

8. References

[1]Roy, C., McWherter-Payne, M., Salari, K. 2002, RANS simulations of a simplified Tractor/Trailer Geometry, UEF.

[2]McCallen R., Couch R., Hsu J., Browand F., Hammache M., Leonard A., Brady M., Salari K., Rutledge W., Ross J., Storms B., Heineck JT., Driver D., Bell J., Zilliac G. 1999, Progress in reducing aerodynamic drag for higher efficiency of heavy duty trucks (class 7-8). SAE Paper 1999-01-223.

[3]Tennekes, H. and Lumley, J. L. 1972 *A first Course in Turbulence*, MIT Press, Cambridge, MA.

[4]Townsend, A. A. 1976 *The Structure of Turbulent Shear Flow*, Cambridge U. Press, Cambridge, UK.

[5]Logan, J. D. 1978 *Applied Mathematics*, Wiley, NY.

[6]Haberman, R. 1983 *Elementary Applied Partial Differential Equations with Fourier Series and Boundary value Problems*, Prentice Hall, Englewood Cliffs, NJ.

[7]Keeney, J. F. and Keeping E. S. 1951 *Mathematics of Statistics Pt. 2*, 2nd ed. Princeton, NJ, Van Nostrand.

[8]Cramer H. 1957 Mathematical Methods of Statistics, Princeton U. Press, Princeton NJ.

[9]Van Dyke, M. 1975 Perturbation Methods in Fluid Mechanics, Parabolic Press, Stanford, CA.

[10]White, F. M. 1986, *Fluid Mechanics,* McGraw-Hill, NY.

[11]Hughes, W. F and Brighton, J. A.,1991, *Fluid Dynamics*, 2nd ed. McGraw-Hill Inc. NY.

[12]Schlichting, H. 1979, *Boundary Layer Theory*, McGraw-Hill, New York.

[13]Lyn, D. A., Einav, S., Rodi, W. and Park, J-H 1995 A Laser-Doppler velocimetry study of ensemble averaged characteristics of the turbulent near wake of

a square cylinder, *Journal of Fluid Mechanics*, 304, pp. 285-319.
[14]Milne-Thomson, L. M. 1968 *Theoretical Hydrodynamics*, Macmillan, NY.

9. Nomenclature

a_i	=	Charlier Series constants
A	=	Velocity solution constant
A_c	=	Cross-sectional area
B	=	Length scale solution constant
C_D	=	Drag coefficient
const	=	Unspecified constant value
g	=	Self-similar eddy viscosity variable
l	=	Turbulent wake lengthscale
R_T	=	Turbulent Reynolds number
U	=	Streamwise Reynolds averaged velocity
u	=	Streamwise turbulent fluctuating component
v	=	Cross-stream turbulent fluctuating component
x	=	Streamwise spatial coordinate
y	=	Cross-stream spatial coordinate
α	=	Defined variable, see equation (10)
θ	=	Momentum thickness
ξ	=	Dim. streamise spatial coord.

Subscripts/supercripts

0	=	Free stream
s	=	Centerline maximum
--- (bar)	=	Reynolds averaged operator
‘	=	Ordinary differential operator
*	=	Dimensionless quantity

9. Appendix I: Potential Flow Over a Semi-infinite Body with a Step

Although a simplified, step function approach was taken with flow over a square cylinder, it is possible to analyze the potential flow over a step in a semi-infinite space.

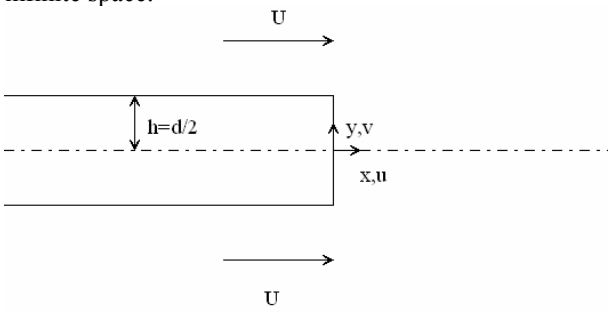

Figure A.1.1 Schematic for 2-d flow over a semi-infinite step

The method (following Milne-Thompson[14]) is based upon the complex potential and the famous Schwarz-Christoffel transformation method. In brief the method involves using the Schwarz-Christoffel transformation to carry the physical problem from the complex (z=x+iy) “z” plane in to the computationally simple (complex) ζ plane. The problem is then solved using superposition of elementary potential functions in the ζ plane to obtain the associated complex potential where $w = \phi + i\psi$. The construction. In general, one can obtain (more or less, the solutions are almost always implicit and in terms of quadratures) closed form solutions for the associated flow field. Following Milne-Thompson, we write:

$$z = \frac{h}{\pi}\left((\zeta^2 - 1) + \cosh^{-1}\zeta\right)$$

$$w = \frac{hU}{\pi}\zeta \qquad \text{(A.1.1)}$$

A more useful form can be obtained by introducing the variable, t where $\zeta = \cosh t$. Thus, in terms of the new variables we write:

$$z = \frac{h}{\pi}\left(t + \sinh t\right)$$

$$w = \frac{hU}{\pi}\cosh t \qquad \text{(A.1.2)}$$

Computing the velocity field from equation (A.1.2) by differentiating since $V = u - iv = -\frac{dw}{dz}$ and $V = \frac{dw}{dt}\frac{dt}{dz}$. Computing the required terms we obtain:

$$\frac{dw}{dt} = \frac{hU}{\pi}\sinh t$$

$$\frac{dt}{dz} = \frac{\pi}{h}\left(1 + \cosh t\right)^{-1} \qquad \text{(A.1.3)}$$

and

$$V = U\frac{\sinh t}{(1+\cosh t)} = U\tanh\left(\frac{t}{2}\right) \qquad \text{(A.1.4)}$$

From equation (A.1.2) we approximate that $z = \frac{2ht}{\pi} + ..O(t^3)$ so that the streamwise velocity is approximated by:

$$u = \mathrm{Re}\left(U\tanh(\frac{\pi z}{4})\right) = U\frac{\sinh\left(\frac{\pi}{2}\frac{x}{h}\right)}{\cosh\left(\frac{\pi}{2}\frac{x}{h}\right)+\cos\left(\frac{\pi}{2}\frac{y}{h}\right)} \qquad \text{(A.1.5)}$$

Note that the fundamental nature of this problem makes it of sufficient interest, that it is appropriate to perform a numerical solution in support of the 2-d analysis. A 2-d problem is shown in figure A.1.1 This solution is for a dimensionless step height, h/L_{domain}=1/10. Notice that there is good agreement between the analytical solution and the numerical problem.

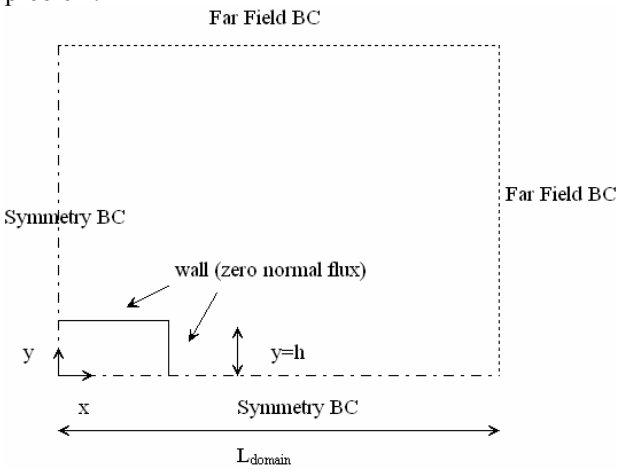

(a) Schematic diagram

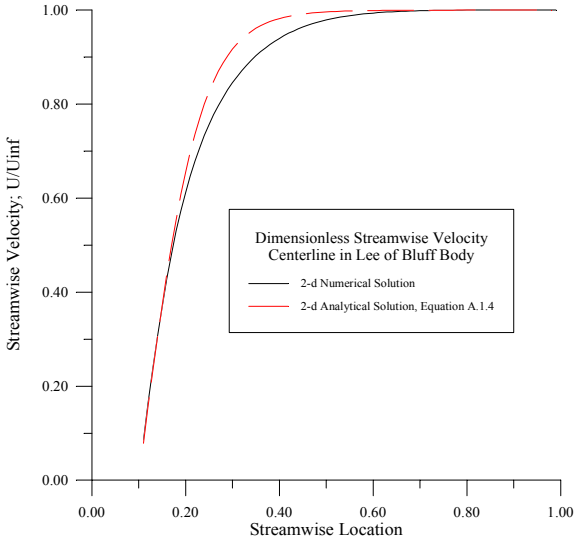

(b) Results

Figure A.1.1 2-d flow over a semi-infinite body with a step computed using analytical and numerical arguments. Dimensionless step height is 0.1, h/L_{domain}.

A second problem of interest is associated with the potential flow over a finite body. We can compute this flow by making several limited modifications to the preceding problem. The schematic diagram of this problem as well as the streamwise velocity directly behind the body is given in figure A.1.3. Notice the good agreement between the semi-infinite models and the finite model.

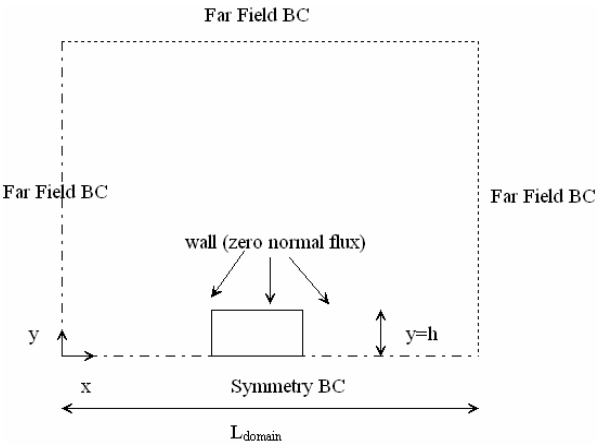

(a) Schematic diagram

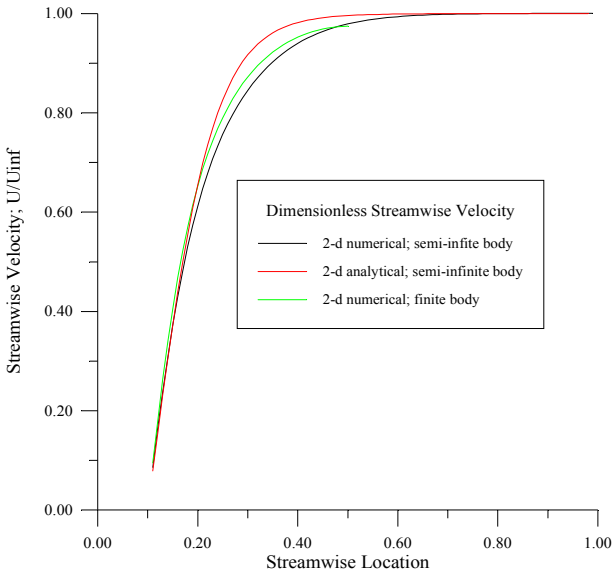

(b) Results

Figure A.1.3 Potential flow over a finite 2-d body. Note, that there is little difference between the semi-infinite and infinite problems.